

Towards time-dependent, non-equilibrium charge-transfer force fields

Contact electrification and history-dependent dissociation limits

Wolf B. Dapp¹ and Martin H. Müser^{1,2} ^a

¹ Jülich Supercomputing Centre, Institute for Advanced Simulation, FZ Jülich, 52425 Jülich, Germany

² Department of Materials Science and Engineering, Universität des Saarlandes, 66123 Saarbrücken, Germany

the date of receipt and acceptance should be inserted later

Abstract. Force fields uniquely assign interatomic forces for a given set of atomic coordinates. The underlying assumption is that electrons are in their quantum-mechanical ground state or in thermal equilibrium. However, there is an abundance of cases where this is unjustified because the system is only locally in equilibrium. In particular, the fractional charges of atoms, clusters, or solids tend to not only depend on atomic positions but also on how the system reached its state. For example, the charge of an isolated solid – and thus the forces between atoms in that solid – usually depends on the counterbody with which it has last formed contact. Similarly, the charge of an atom, resulting from the dissociation of a molecule, can differ for different solvents in which the dissociation took place. In this paper we demonstrate that such charge-transfer history effects can be accounted for by assigning discrete oxidation states to atoms. With our method, an atom can donate an integer charge to another, nearby atom to change its oxidation state as in a redox reaction. In addition to integer charges, atoms can exchange “partial charges” which are determined with the split charge equilibration method.

PACS. 34.20.Cf Interatomic potentials and forces – 02.70.Ns Molecular dynamics and particle methods

1 Introduction

As an illustration of a system with history-dependent forces consider the following thought experiment: a neutral gold cluster and a neutral sodium cluster are prepared separately and placed at a large separation in a UHV chamber. The two clusters are then moved to close proximity and separated later in such a way that no atoms have transferred between the clusters. Since sodium has the smaller work function, the gold cluster will have picked up electrons from the sodium cluster after the separation. As a result, the two final clusters will carry opposite charge and thus attract each other through a long-range Coulomb force, which was not there initially. This implies that the atomic interactions between – but also within – the two clusters differ between the initial and the final state. This is the case even if we allow for a demon enforcing the atoms to take identical positions at the beginning and at the end. Current force fields are intrinsically unable to reflect such changes in the atomic interactions, because they assign to each atomic configuration an unambiguous set of forces.

Even charge equilibration (QE) or charge-transfer methods [1,2] fail to describe the electrostatic fields that

arise due to the contact-induced charge transfer. They determine fractional charges as single-valued (vector) functions of the instantaneous atomic coordinates just like conventional density functional theory provides a unique electronic charge densities for a given atomic configuration. While attempts to incorporate time dependence into density functional theory-based approaches to the electronic state are thriving [3], virtually no attention has been paid to the question how to tackle history-dependent fractional charges with classical force fields. Being able to do so would not only prove useful to reproduce non-equilibrium charge transfer processes as they occur in our thought experiment. It might also become possible to simulate many other systems and processes which are not amenable to simulations based on current force-fields, or contain too many particles for calculations necessitating the solution of time-dependent quantum mechanics. One such example, discussed in this work, is the dissociation of a NaCl molecule in solvents, which can result in neutral or singly-charged dissociation products depending on the solvent polarity. Another example, which we discuss in detail in a separate work, is the discharge of a small-scale battery [4].

The proper description of electron transfer upon contact formation is a crucial aspect in the all-atom simulation of the discharge of a battery, since closing and opening of an electric switch involves the formation and the break-

^a e-mail: martin.mueser@mx.uni-saarland.de

ing of a (mechanical) contact between two solid bodies. This can be seen in the following discussion. Consider a battery which is attached to an electric circuit with an Ohmic resistor and an initially open switch. When the switch is closed, a demon manages to keep all atoms near their initial positions. After some electric current has flown through the external wire, the switch is opened again. Although no atom has moved substantially inside the battery, the charge distribution, or, more generally speaking, the electronic state can have changed significantly, because many electrons, i.e., integer charges, have moved through the wire and the external Ohmic resistance. To summarize, current force-fields or DFT-based methods can predict neither the voltage of a Galvanic cell nor its time dependence during discharge, because they are intrinsically unable to describe out-of-equilibrium processes as they occur in our thought experiment of the contact formation between two metals, e.g., the closing of a switch.

Integer charge transfer between atoms, molecules, clusters, or solids is not only at the root of contact electrification but also of many other processes, in particular of any redox reaction. Most redox reactions can be understood in quite simple terms and experienced chemists can easily make accurate predictions for the outcome of a redox reaction. Yet, surprisingly little work has been devoted to cast this chemical intuition into a quantitative framework that does not necessitate the solution of the Schrödinger or related equations. However, in principle, it should be possible to design an approach that does not only reflect chemical intuition but also describes the energetics of the reactants and the products of a redox reaction with a precision as high as that of accurate force fields designed for non-reactive systems. To date, force fields require different parameterizations for the products and the reactants of a redox reaction. Even force fields designed to describe chemical reactions, such as ReaxFF [5], fail to account for the charge transfer effects discussed in the context of the contact formation between two clusters and the discharge of a battery. A redox reaction implies a quasi-discontinuous change of the electronic state [6], which cannot be captured by any force field that assumes a continuous evolution of interatomic forces with atomic coordinates.

In this paper we explore the suggestion that introducing oxidation states into a charge-transfer approach makes it possible to capture history dependence in classical force fields and to model (non-equilibrium) redox reactions [7]. Our intent is to demonstrate a proof of concept rather than to model a specific system with high accuracy. In this first attempt, we focus our attention on the thought experiment discussed at the beginning of the introduction. In a future publication we will demonstrate that all-atom simulations of batteries (based on the methodology developed herein) reproduce non-trivial observations, such as the existence of a voltage plateau during discharge of the battery for small discharge rates.

The remainder of this work is organized as follows: In Section 2 we summarize the split-charge equilibration (SQE) model [8], which we used as a basis for our study.

This includes a discussion of the original method as well as its extension to “redoxSQE,” in which oxidation states can be changed. In Section 3 we demonstrate that redoxSQE indeed captures the time dependence of interactions between molecules as discussed in our first thought experiment. Conclusions are drawn in Section 4.

2 Method

2.1 The split-charge equilibration method

Charge equilibration methods are based on the minimization of an expression reflecting the energy as a function of the charge distribution in an atomic system [1,2]. In this work we use the split-charge model [8]:

$$V = \sum_i \left(\frac{\kappa_i}{2} Q_i^2 + \chi_i Q_i \right) + \sum_{i,j < i} \left(\frac{\kappa_{ij}}{2} q_{ij}^2 + J_{ij} Q_i Q_j \right). \quad (1)$$

Here, Q_i is the (possibly fractional) charge of atom i . Its chemical hardness and electronegativity are denoted by κ_i and χ_i , respectively. J_{ij} reflects the distance-dependent Coulomb interaction between two atoms, which we do not screen at short distances, i.e., $J_{ij} \equiv 1/r_{ij}$ in this study, r_{ij} being the distance between two atoms. The term q_{ij} denotes a partial charge, or “split charge”, donated from atom j to atom i . It is antisymmetric in the indices, i.e., $q_{ij} = -q_{ji}$. The net charge of an atom in the formulation proposed in reference [7] then reads:

$$Q_i = n_i e + \sum_j q_{ij}, \quad (2)$$

where n_i is the (formal) oxidation state and e the elementary charge. The term κ_{ij} , which is distance dependent (and should usually also be environment dependent), is called the bond hardness. It is inversely proportional to the polarizability of the bond connecting two atoms. In the condensed phase, the inverse bond hardness associated with nearest neighbors is proportional to the dielectric permittivity [9].

We refer to the original literature for an in-depth discussion and motivation of the SQE model [8,9,7]. However, we summarize some of its properties in this section and compare it to other charge equilibration approaches. In contrast to the traditional purely atom-based charge transfer potentials, i.e., those omitting bond-hardness terms, the SQE model produces the correct dissociation limit of molecules [8,7,10], the (high-frequency) dielectric permittivity does not automatically diverge [9], it shows the correct linear scaling of the polarizability of polymers with increasing chain length [11,12], as well as the correct slight reduction of the dipole of alcohols with increasing length of the fatty tail [13]. Lastly, the chemical hardness of molecules (which one can associate with the band gap of solids) levels off at a finite value rather than to become zero for large atom numbers [7]. In contrast to purely bond-polarizability based models, i.e., approaches excluding the singly-indexed atomic hardness κ_i , SQE shows the

correct scaling of oligomers with decreasing chain length [11], it is not restricted to systems with a dielectric permittivity just slightly above unity [7,9], the chemical hardness of molecules is positive as it should be, rather than negative [7], and it maintains the concept of atomic hardness, which is well motivated from the density functional theory (DFT) formulation of quantum mechanics [14,15,16]. SQE has also been coupled to bond-order potentials describing short-range interactions. Good values were obtained for dipoles and heat of formation for isolated molecules, radial distribution functions of liquids, as well as reasonable energies of oxygenated diamond surfaces [17].

The work on charge transfer models by Verstraelen and coworkers deserves particular mention. They found that SQE outperforms previous charge equilibration approaches in all of their 23 benchmark assessments when applied to a large, systematically chosen set of organic molecules [12]. In a later study [18], they showed that SQE produces good charges and response functions for both isolated silicate and related molecules as well as their condensed ceramic phases, by using an unambiguous and thus transferable parameterization scheme. In contrast, atom-based charge transfer approaches suffered from the usual superlinear scaling of the polarizability. In a theoretical work, Verstraelen *et al.* motivate the combination of bond hardness and atomic hardness with DFT-based considerations [19]. In a recent study [20], they recognized that the original SQE model (i.e., the one in which all oxidation states are set to zero) fails to predict fractional charges and polarizabilities of zwitterionic molecules. Once charges of (formally charged) fragments in (zwitterionic) molecules were constrained to be a positive or negative elementary charge plus a split charge from the atom to which the fragment was bonded, fractional charges turned out to compare well to those deduced from an iterative Hirshfeld partitioning. Their constraint on fragments [20], called SQE+Q⁰, is similar in spirit to redoxSQE, even if atom-based charge-transfer models cannot be extended to fragments in a simple, systematic fashion [21,22].

2.2 Bond hardness and bond breaking

In the phenomenological framework of the SQE model, the value of the bond-hardness terms classifies the nature of the bond between two atoms. A bond between two atoms i and j is called metallic if $\kappa_{ij} = 0$. When two atoms are not bonded, no split charge can be shared, which can be expressed formally with $\kappa_{ij} = \infty$. If κ_{ij} is positive and finite, we classify the bond as dielectric. Of course, conductivity is a collective property rather than a function of the separation between two atoms, and approaches like ours will be unable to capture resonance effects, for instance in molecular-scale electronics. Yet, we are in a position to set up local rules producing the correct macroscopic dielectric response functions when properly parameterized. We feel that this is progress with regards to routinely-used charge equilibration approaches (such as the one employed in ReaxFF) which always yield the response of ideal metals [9,7].

For simplicity, we take the bond hardness as a function solely of the separation between any two atoms — or ions, once we have introduced oxidation states. This first-order approximation will have to be abandoned for material-specific simulations, where one might want to design the bond hardness along the lines of bond-order potentials [23]. A bond shall be broken, i.e., κ_{ij} should diverge, if r_{ij} exceeds the threshold value r_1 . This also implies that atoms i and j no longer share a split charge. (In reality, the polarizability between two distant atoms should never be exactly zero, but decay exponentially as their atomic orbitals cease to overlap.) At short separation ($r_{ij} \leq r_s$), κ_{ij} should move to a value such that a system composed of dimers at the given separation gives the correct dielectric response.

To show the generic features of our model, we use a rather basic model, where the bond hardness is either zero (to reflect traditional charge equilibration approaches) or a unique function of distance. Making $\kappa_{ij}(r_{ij})$ depend on the oxidation state of the atoms does not change the property of the model qualitatively. For a neutral dimer in the redoxSQE description, we set the two atomic oxidation states to zero, or alternatively, to $n_{1,2} = \pm 1$ (so that the net charge of the molecule remains zero).

We adopt the functional form for κ_{ij} similar to the one introduced by Mathieu [10], who already parameterized bond breaking in the split-charge framework. Specifically, we choose:

$$\kappa_{ij} = \begin{cases} \kappa_{ij}^{(p)} & r_{ij} \leq r_s, \\ \kappa_{ij}^{(p)} + \kappa_{ij}^{(0)} \frac{(r_{ij}-r_s)^2}{(r_1-r_{ij})^2} & r_s < r_{ij} < r_1, \\ \infty & r_1 \leq r_{ij}. \end{cases} \quad (3)$$

Here, $\kappa_{ij}^{(p)}$ is the plateau value, which is zero for metals and positive for dielectrics, while $\kappa_{ij}^{(0)}$ is always positive. We do not claim that the functional form in equation (3) is chemically realistic, although Mathieu [10] found quite reasonable trends for fractional charges in the analysis of the homolysis of a variety of organic molecules. That work included results for radicals and transition states, even though the calibration was done on equilibrated structures satisfying the octet rule.

Our diatomic molecule shall be characterized as follows. Atomic hardness: $\kappa_1 = \kappa_2 = 3.5$ (in arbitrary units, which in typical cases should correspond roughly to V/e), and electronegativity: $\chi_{1,2} = \mp 1.5$, i.e., atom 2 (henceforth called the anion) is more electronegative than atom 1, which one could associate with the cation. This choice implies the correct dissociation limit, that is, the energy required to transfer charge between two distant atoms is positive, specifically $\Delta E_{\text{trans}} = 0.5$. Moreover, we choose $r_s = 0$, $r_1 = 2$, $\kappa_{12}^{(p)} = 0$, and $\kappa_{12}^{(0)} = 1/8$. The Coulomb interaction reads $V_C = Q_1 Q_2 / r_{12}$. The split-charge can be calculated by minimizing equation (1) with respect to the split charge q_{12} , i.e.,

$$q_{12} = \frac{\chi_2 + (\kappa_2 - J)n_2 e - \chi_1 - (\kappa_1 - J)n_1 e}{\kappa_1 + \kappa_2 + \kappa_{12} - 2J} \quad (4)$$

We consider neutral systems, i.e., $n_1 = -n_2$. For the discussion of charged systems and molecular hardness, we refer to reference [7].

We add a short-range two-body interaction energy to the split-charge related energies. For reasons of simplicity we use a standard Lennard-Jones potential:

$$V_{\text{LJ}}(r) = 4\epsilon \left\{ \left(\frac{\sigma}{r} \right)^{12} - \left(\frac{\sigma}{r} \right)^6 \right\}, \quad (5)$$

where $\epsilon = \sigma = 1$ are chosen. Here, a typical value for σ would be 2\AA . We abstain from adjusting any interaction parameters for different oxidation states, even if this level of simplicity is probably not tenable for realistic parameterizations. The resulting charges on atom 1 and the total energy for different oxidation states are shown in Figure 1.

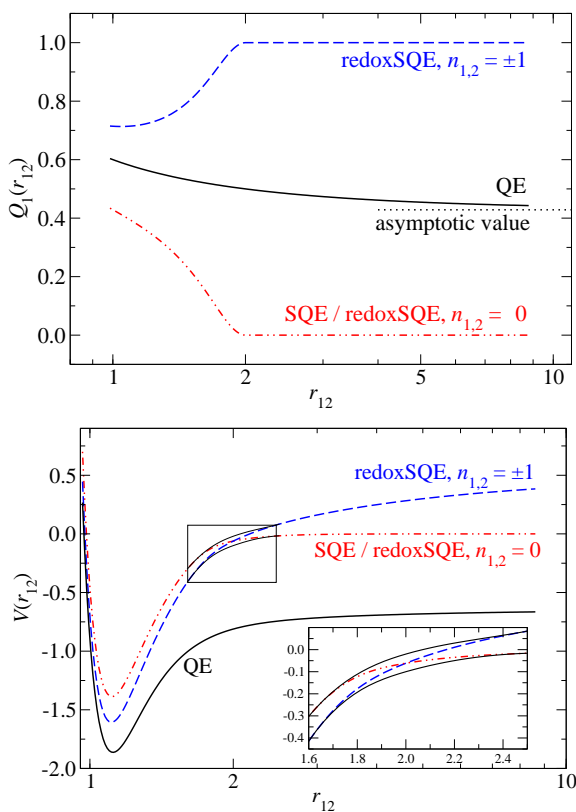


Fig. 1. (Color online) In both graphs, two different oxidation state configurations are considered as well as the conventional charge equilibration approach (QE). **Top:** charge Q_1 of the “cation” as a function of the interatomic distance r_{12} for different computational approaches. The dotted black line is the charge on the electropositive atom predicted by the QE method for an infinite separation. **Bottom:** energy V_{12} of the diatomic molecule as a function of the interatomic distance. The short black lines in the bottom graph illustrate the functional dependence of the energy of the quantum-mechanical ground state and the first excited state on the interatomic distance.

The top panel of Figure 1 illustrates that conventional QE ($\kappa_{ij} \equiv 0$, choice of n_1 irrelevant for neutral systems)

produces fractional charges on the two atoms even when they are distant. At infinite separations, the charge on the electropositive atom levels off at a finite value $(\chi_2 - \chi_1)/(\kappa_1 + \kappa_2) \approx 0.43$, indicated by the black dotted line. In redoxSQE however, the two atoms are either neutral, or each one carries an integer charge of opposite sign in the dissociation limit, owing to the diverging bond hardness.

In the bottom part of Figure 1, we point out that the two redoxSQE energy curves with different values for n_1 cross. At short separation, the system benefits if it transfers a negative integer charge to the anion, while both atoms are preferably neutral in the dissociation limit. Qualitatively, the behavior of the two curves is similar to those obtained from full quantum-mechanical potential energies of ground states and first excited states, except near the transition region. There, the two curves would not cross but the $n_1 = 1$ curve would smoothly evolve into the $n_1 = 0$ curve and vice versa (as sketched by the short black lines). We note that the crossing of the two levels does not have to occur at r_1 , but that both existence and location of the crossing point depend on the choice of parameters. Moreover, we note that the asymptotic behavior of the $n_{1,2} = \pm 1$ curve for large r_{12} reflects the Coulomb attraction between two opposite, integer charges as well as the energy ΔE_{trans} required to ionize atom 1 and donate the electron to atom 2.

2.3 Some quantitative analysis for NaCl

It is beyond the scope of this work to perform a full parameterization of the method to real materials using quantum-chemical data. However, as demonstration of the applicability of the method to a real system, we performed MP2 calculations of the dissociation of an NaCl dimer in Gaussian [24], with the basis function set 6-311G+. These calculations used the restricted Hartree-Fock method, which enforces closed electron shells for the dissociation products and causes the system upon separation to move onto the “excited” energy curve in a Landau-Zener picture. For NaCl, this implies that $n_{\text{Na,Cl}} = \pm 1$, and does not allow for a neutral dissociation, even in vacuum. The result is an energy curve very similar to that for the charged dissociation of a generic dimer (dashed blue line in Figure 1, bottom panel).

To the MP2 energy curve we fit two models. First, a Born-Mayer potential [25] with a simple unscreened (fixed-charge) Coulomb interaction, and two free parameters, in the repulsive short-range term. Figure 2 (bottom panel) reveals that this simple, purely two-body potential fits the data surprisingly well. This result is fortuitous in parts, because the model uses a simple unscreened Coulomb interaction. Allowing for screening did not improve the results.

The second model uses the redoxSQE potential with a screened Coulomb interaction for short separations, and self-consistent charges. The ionic dissociation necessitates determining hardness and electronegativity for the ions and not the neutral atoms. We obtain the ionization energy of Cl^- and the electron affinity of Na^+ from consis-

tent MP2 calculations for isolated atom/ions. Since the electron affinity of the Cl anion is not defined, we have to work with an effective value. We obtain one additional constraint by setting the electronegativity difference equal to the screened Coulomb energy close to where the electrostatic potential (ESP) charges derived from the MP2 calculations cross the $Q_{\text{Na}}/e = 1$ line. These three values are sufficient to gauge the needed single-ion parameter combinations ($\kappa_{\text{Cl}^-} + \kappa_{\text{Na}^+}$) and ($\chi_{\text{Cl}^-} - \chi_{\text{Na}^+}$).

To reflect screening we replaced the $1/r$ Coulomb potential with a $\tanh(r/a_{\text{scr}})/r$ dependence, which we found to be very similar to Slater-type orbital screening. At the present stage of development, we treat a_{scr} as an adjustable parameter. We find that, as argued in Section 2.2, a simple $\kappa_{\text{Na}^+\text{Cl}^-} \propto \exp(r/a_b)$ relation is sufficient to reproduce the ESP charges from the MP2 calculation at all distances, see top panel of Figure 2.

Having determined those parameters, we fit the energy curve with two free parameters, namely those in the repulsive short-range term, as in the Born-Mayer case. The fit of the redoxSQE model to the data is also very good — the error is $\lesssim 4\%$ of the binding energy everywhere. We note that while Born-Mayer uses only two fit parameters, we have a total of five adjustable parameters. However, in our approach, we reproduce the ESP charges, which are assumed to be constant in Born-Mayer. Moreover, the resulting values for the fit parameters are physically meaningful. For example, we obtain a combined ionic hardness of $33 \text{ V}/e$, which is similar in magnitude to the experimental hardness of the sodium cation of $42 \text{ V}/e$ (the Cl anion contributes very little, because it is chemically soft). The bond hardness, evaluated at the NaCl distance in the rocksalt crystal, is $57 \text{ V}/e$. Given the relation for the high-frequency dielectric permittivity for rock salt equation (27) in reference [9] this would produce a value of $\epsilon_r = 2.1$, which is close to the experimental value of $\epsilon_r = 2.25$.

Note that the charge on the sodium atom resembles the behavior seen in Figure 1 (top panel) in that it decreases from very small separations (as in the QE case), transitions through a rise at intermediate distances, and finally levels off to $+1$ at large separations (the detailed shape of the curve depends on the choice of κ_{ij} , which in the generic case was chosen a divergent rational function, while $\kappa_{\text{Na}^+\text{Cl}^-}$ increases only exponentially with separation). A reduction of the Born effective charge with increasing pressure is also seen in DFT calculations of solid MgO [26], from $+2$ at zero pressure to ≈ 1.65 at $\approx 800 \text{ GPa}$. A similar result can also be derived from Raman scattering data on ZnO [27], from $+1$ at zero pressure to ≈ 0.96 at $\approx 5.5 \text{ GPa}$. Such reductions can only be achieved with redoxSQE and the inclusion of oxidation states, as conventional SQE (including QE) automatically predicts a monotonic *increase* in charge upon compression. This is because the increasing Coulomb interaction upon compression always increases the split charge when the reference state consists of neutral atoms.

In future work, we will carry out a more detailed study on the transferability of the redoxSQE parameters.

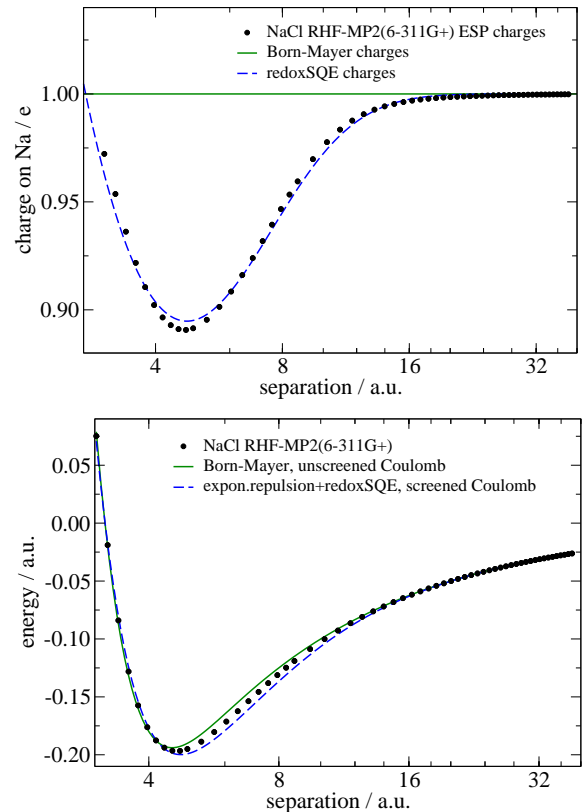


Fig. 2. (Color online) **Top:** ESP charges on sodium from RHF-MP2(6-311G+) calculations with Gaussian of the dissociation of NaCl in vacuum, as well the charges predicted by the redoxSQE model. The Born-Mayer model uses constant charges ± 1 . The MP2 data also sets the functional form of $\kappa_{\text{Na}^+\text{Cl}^-}$. **Bottom:** Fits to MP2 energy data. A simple Born-Mayer potential with an unscreened Coulomb interaction and constant charges fits fortuitously well. The redoxSQE model with a screened Coulomb interaction fits the data comparably well. Both models have two free parameters for the repulsive term. In addition the redoxSQE model uses parameters determined from MP2 calculations for isolated Na/Na⁺ and Cl/Cl⁻ as well as the ESP charges of an Na⁺Cl⁻ dimer.

2.4 Assigning oxidation states

Before addressing how to design dynamics for the transition between the $n_{1,2} = \pm 1$ and the $n_{1,2} = 0$ surface, we wish to comment on the asymptotic behavior of interatomic forces near r_1 . Since q minimizes the potential energy, the interatomic force reads, in the generic two-body problem considered here:

$$\mathbf{F}(r_{12}) = \mathbf{F}_{\text{LJ}}(r_{12}) + \mathbf{F}_{\text{C}}(r_{12}) - q_{12}^2 \nabla \kappa_{12}(r_{12}). \quad (6)$$

In addition to the Lennard-Jones force, \mathbf{F}_{LJ} , and Coulomb force between (point-) charges, \mathbf{F}_{C} , an additional term arises as a result of the distance dependence in the bond hardness. We disregard possible environment-dependent corrections to atomic hardness and electronegativity. If we now assume that κ_{ij} diverges with a power law $1/(r_1 - r_{12})^{\alpha_1}$,

the absolute value of the additional force term scales as $q_{12}^2/(r_1 - r_{12})^{\alpha_1+1}$. The split charges themselves scale as $q_{ij} \propto 1/\kappa_{ij}$ when r_{ij} approaches r_1 . Thus, the extra contribution to the force originating from the bond-hardness terms becomes

$$-q_{12}^2 \nabla \kappa_{12}(r_{12}) \propto (r_1 - r_{12})^{\alpha_1-1}. \quad (7)$$

Choosing $0 < \alpha_1 < 1$ would lead to an integrable singularity in the force, so that the bond could be broken with finite energy. However, a numerical implementation has the high risk of leading to unstable simulations. For $\alpha_1 = 1$, the force is discontinuous at r_1 , which implies that the usually used symplectic (Verlet) integration algorithms would no longer be strictly energy conserving (this would be roughly equivalent to cutting off potentials at finite distances without smoothing the potential). Our choice of $\alpha_1 = 2$ leads to a discontinuity only in the first derivative of the force. This means that the second derivative is divergent at isolated points so that symplectic integrators might still show very small drifts, which should nevertheless be unnoticeable in practice.

The behavior for the discontinuity in the force-distance curve at the short-range cutoff can be discussed in similar terms as that at large distances. Now, q does not necessarily tend to zero and must therefore be assumed to be finite at $r = r_s$. Thus, assuming that the “excess” hardness, i.e., $\kappa_{12} - \kappa_{12}^{(0)}$ increases with $(r - r_s)^{\alpha_s} \Theta(r - r_s)$, one obtains a discontinuous force at r_s for $\alpha_s = 1$ and a discontinuity in the first derivative of the force for $\alpha_s = 2$. Here, Θ is the Heaviside step function.

Simulating the dissociation of molecules, clusters, or solids necessitates rules for the change of the oxidation state of individual atoms – or at least of fragments. The feature of the redoxSQE model that we explore in this work is that it allows for integer charge transfer (ICT) besides the exchange of partial charges across bonds between two atoms. This section explains our implementation of such ICTs. First, however, we motivate the rules by performing an asymptotic analysis of a charge transfer process, which is similar in spirit to the thought experiments discussed in the introduction.

Consider a chlorine atom close to a surface of metallic sodium in UHV, as illustrated in Figure 3(a). Initially the Cl atom is close to the Na metal and is moved adiabatically to a distant position. Straight from the onset, the sodium cluster will have donated an electron to chlorine. At no point in time will the chlorine be able to reduce its energy by donating its extra electron to the sodium, because the electron affinity of chlorine exceeds the work function of solid sodium. Thus, the final charge of the Cl atom will be -1 and that of the Na cluster +1.

In contrast, if we reach the final configuration through the process shown in Figure 3(b), the chlorine will remain neutral on experimentally relevant time scales. The reason is that an (adiabatic) dissociation of the NaCl dimer leads to two neutral atoms, because the ionization energy of Na exceeds the electron affinity of Cl. Thus, the final states for the two cases differ. We stress that we did not assume any “extreme” conditions, such as high shear rates

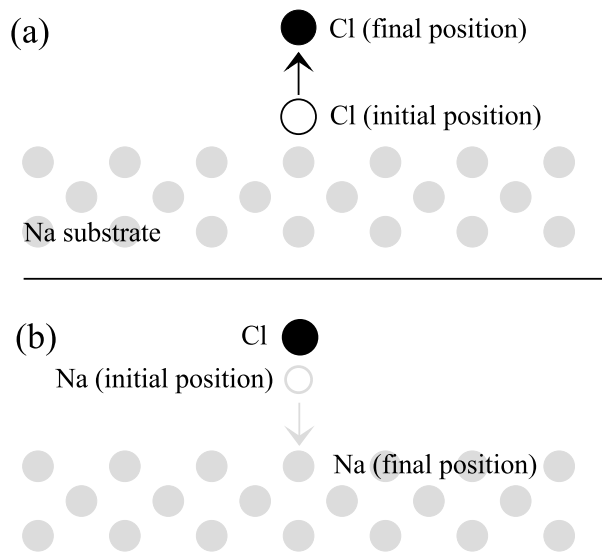


Fig. 3. Schematic illustration of the history dependence of atomic charges. The final nuclear configurations in (a) and (b) are identical. However, in (a), the chlorine atom has initially resided on the surface of the metal cluster so that its final charge will be a negative elementary charge. In (b), an NaCl molecule is dissociated first leading to two neutral atoms. When the Na is introduced into the bulk substrate, the Cl is too distant to receive an electron from the bulk metal on relevant time scales. The different outcome despite identical final positions arises because the electron affinity of chlorine exceeds the work function of metallic sodium but is smaller than the ionization energy of atomic sodium.

or pressures, as they typically occur at microscopic contact points between two rubbing solids.

Determining the precise rates of electron transfer reactions is a mature field of research [6]. The transfer of electrons between atoms can occur with non-negligible probabilities on time scales shorter than a molecular dynamics time step when two atoms are not too distant from one another. Once they have moved away from one another, the rates decrease exponentially with separation so that they eventually become negligible even over extended periods of time. In many cases, such as the desorption/dissociation of a Cl atom from sodium discussed in this section, the outcome does not depend sensitively on the time when this transfer has occurred. In our current example, the precise electron tunneling rate would only matter if the molecular dissociation in case (b) occurred at an “intermediate” distance from the surface. In all other cases, it would suffice to have an algorithm producing approximate average rates for the electron transfer process.

To mimic electron tunneling dynamics we proceed as follows: at each time step, we select all “relevant” dielectric bonds. As mentioned before, a bond is called dielectric if two atoms are sufficiently close together to share a split charge, but not close enough to have a vanishing bond hardness. Which pairs of atoms are classified as sharing a relevant bond depends on the problem of inter-

est. In the current example, it would only be the bond between the chlorine atom and one sodium atom if their distance is small — or the bonds to several atoms at the bulk sodium surface. In the contact formation between two solids discussed in the introduction, relevant bonds would be the ones between pairs of atoms from different metal clusters. Non-relevant dielectric bonds are those where electron hopping can be neglected, for example, between two atoms belonging to the same dielectric material, which we assume to be non-conducting, or two atoms far apart (with a separation $> r_1$). In general, the number of relevant bonds should be $< gNZ$, where N is the number of atoms, Z the average coordination number, and $c^2 < g < c$. Here, c denotes the fraction of atoms capable of redox reactions. One would expect $g \propto c^2$ if the redox-active atoms are perfectly dissolved in a redox-inert solvent, while $g \lesssim c$ if they do not dissolve at all.

Once a bond has been identified as relevant, we examine certain additional conditions to determine whether to attempt an ICT. Some conditions that could stifle an ICT are physical constraints. An example is the ability of a donor to give an electron (e.g., H^+ cannot donate an electron), or the possibility for an acceptor to receive it (e.g., it is exceedingly unlikely that Cl^- accepts an electron). Second, in order to reflect electron transfer probabilities, we require that the product of time step size and estimated transfer rate is greater than a random number between zero and one. (In chemically realistic simulations, the transfer rate must be determined from quantum-mechanical calculations [28].) In addition, in order to alleviate a bias introduced by the order in which we query bonds, we draw an additional random number and only proceed with the trial ICT if it exceeds some threshold (for instance 0.9, to attempt an ICT only every tenth MD time step). An easy way to avoid bias altogether is to pick the trial-ICT bonds at random from the pool of relevant bonds. For the examples studied herein, this turned out unnecessary, which we ascertain from the observation that the symmetry of the problem was maintained.

If all conditions are met, we make a trial ICT. This involves changing the oxidation state of the two bonded partners, incrementing one, and decrementing the other by 1, with the direction of transfer set by the sign of the current split charge between the two partners. We then re-equilibrate all split charges within some cutoff radius R^{opt} . This approach implicitly assumes that the electronic response to a discontinuous change in the electric field, as it is brought about by the ICT, is faster than the inertial response of the atoms, which is traced by an MD time step.

In our current, developmental implementation $R^{\text{opt}} = \infty$, which means that all split charges are updated in each trial move. This makes each individual trial ICT an expensive $\mathcal{O}(N^2)$ operation and thus, a full sweep through the system is $\mathcal{O}(gZN^3)$. Assuming that *all* split charges react (instantaneously) to a changed electric field, is similar to saying that *all molecular orbitals of the system will be modified during an (electron transfer) reaction* [6]. However, it should often be possible to turn the trial ICTs

into local operations with bounded errors [7], by choosing a finite cutoff radius. The reason is that the change in the split charges induced by the redox move decreases very quickly with increasing distance to the location of the electron transfer.

After the equilibration we calculate the total potential energy of the system, except for the charge-independent short-range terms. Generally, atoms that changed their oxidation states would have differing short-range interactions with their neighbors as well. For instance, the chlorine anion is significantly larger than a neutral chlorine atom. For now, we neglect this change. If the energy after the change of oxidation state and subsequent split-charge equilibration is equal to or below what it was before, the ICT is accepted, otherwise it is rejected. In other words: for each atomic configuration, knowledge of the set of oxidation states allows one to deduce on which (Landau-Zener-type) energy surface the system is currently evolving. An ICT allows to hop from one surface to another, lower one. A natural alternative to this minimal energy procedure, which keeps the electrons close to their ground states, would be to apply the Metropolis algorithm. In case of a rejection, we undo the changes in oxidation state and restore all split charges to their values before the trial ICT. If a move is accepted, the next relevant bond is examined, on the basis of the modified charge distribution in the system. When this process is exhausted, the new charge distribution is used for the force calculation for the next MD step.

Note that the described procedure is not energy conserving. We implicitly assume that the excess energy liberated by the electron transfer escapes as radiation. It is not difficult to design a modified ICT that is radiation-free, for instance by adding the released energy to the kinetic energy of the two participating atoms (and modify the acceptance criterion of a trial ICT accordingly), for instance, as in reference [28]. We leave this extension for future work.

ICTs across metallic bonds ($\kappa_{ij} \equiv 0$) are unnecessary, because backflow of the split charge q_{ij} exactly compensates the integer charge transfer. Atomic charges and total energies are unaffected in this case, so that every trial move would be accepted, but no interatomic force would change. Rather than assigning oxidation states to individual atoms sharing a metallic bond, it would be more meaningful to assign them to connected metal clusters. However, in many cases, such as the ones discussed in this section, the overhead of constructing clusters can be avoided.

3 Case studies

3.1 Contact formation between metals

The mechanism of contact electrification between two metals is well established [29]. Electrons transfer from the metal having the smaller work function to that with the larger one. The resulting charged solids then have a reduced difference of their work functions and the charge

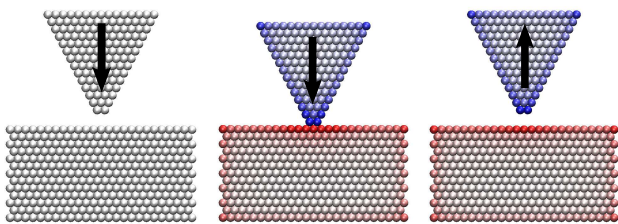


Fig. 4. Visualization of the contact electrification of a metal tip and a metal substrate. Red and blue indicate, respectively, the amount of negative and positive charge per atom. Initially neither solid is charged. When they are brought to close proximity, charge can transfer between them such that negative charge flows from the metal with the small work function to that with the large work function. After the solids have been separated, no more charge can flow.

transfer eventually comes to a stop. Of course, the amount of transferred charge is affected by electrostatics, i.e., by the total capacitance of the two metals and by the rate at which the two metals are pulled apart. Thus, while the *amount* of transferred charge may be difficult to predict theoretically, the *direction* of charge flow between initially neutral *metals* is entirely determined by their work functions. Therefore, metals can be arranged in a well-defined fashion into the triboelectric series [29,30], which lists materials closer to the top (bottom) the more it has the propensity to have attracted negative (positive) charge after having touched or rubbed against a counter body.

Figure 4 demonstrates that our model reproduces the qualitative features of charge transfer between metals. It shows a tip which is brought into close contact with a substrate and then separated again. The clusters are initially neutral; however, during contact, charge can transfer, and remain (to some extent) on the clusters after separation. The charge distribution mainly lives on the surface of the clusters, as expected for metals, because this minimizes the (repulsive) electrostatic energy.

In the simulations for Figure 4, the center of mass of the tip was moved by a small increment at each time step, and all atoms within the tip were kept fixed relative to its center-of-mass. Within each solid the bond hardness was set to zero. Bonds between atoms belonging to different solids turned dielectric — and could thus share a split charge — when their separation was below the threshold r_1 . For the calculations shown here, a trial ITC was made in each dielectric bond with a trial rate inversely proportional to the bond hardness. The electron tunneling rate therefore also has this proportionality, i.e., it decreases quadratically with increasing separation between the clusters, and vanishes at $r_{ij} = r_1$. One can certainly envision other rules for the attempt frequency, for instance an exponential decrease with distance, which corresponds more closely to an exponentially decreasing electron tunneling rate. However, the details of such rules do not affect the results in a qualitative fashion, which is why we abstained from “fine tuning” the parameters.

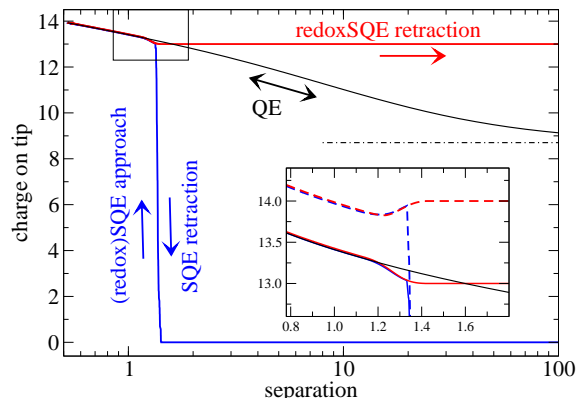


Fig. 5. Charge of the electropositive metal cluster from Figure 4 as a function of separation. The blue line represents the charge curve using the original SQE method during both approach *and* retraction. Using the redoxSQE formalism, the charge follows the blue curve during approach, but the red one during retraction. The black line reflects the results from a traditional charge equilibration method. The dot-dashed black line corresponds to the charge transfer in the QE model when tip and substrate are infinitely far apart. **Inset:** blow-up of the redoxSQE charge-distance curve. The dashed lines represent a simulation in which the electronegativity difference between tip and substrate atoms was increased by $\approx 10\%$ with respect to the original data.

We repeated the same calculation with a pure QE model, in which (split) charge can flow freely between all atoms. As a consequence, the charge distribution is a unique function of the distance between the two parts, in a similar fashion as in the formation and breaking of a diatomic molecule in Figure 1. The results for the metallic tip-substrate system are shown in Figure 5. The charge transfer is driven by the electronegativity difference and opposed by the generation of an electrostatic field around each metal cluster, i.e., by the (inverse) capacitance of the two metal pieces, which is predominantly a function of the shape of tip and substrate, and, for small clusters, also a function of the atomic hardness.

The inset of Figure 5 reveals that the charge on the electropositive tip does not necessarily decrease monotonically with the separation between tip and substrate. The final charge tends to be the closest integer value to the charge at a separation $r \lesssim r_1$, which can result in a rounding-up of the charge as in the $n_1 = 1$ case in the top panels of Figure 1 and 2. Conversely, if the next integer charge is more easily reached by rounding down, the charge behaves more like in the $n_{1,2} = 0$ case of Figure 1.

3.2 Contact formation between dielectrics

The charge transfer between dielectrics is much less well understood than that between metals. Competing views are that rubbing or other contact-dynamics induced charging occurs *predominantly* through electron transfer (potentially via gap surface states) [31], proton transfer [30], or the exchange of hydroxide or other ions [32]. Unlike

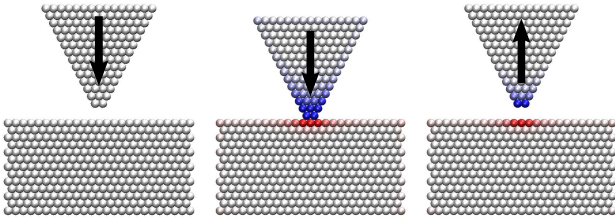


Fig. 6. Similar to Figure 4. However, this time, the bonds within each solid are modeled as dielectric. This prevents the charge from delocalizing significantly.

metals, dielectrics cannot be arranged in a unambiguous fashion into a triboelectric series. In some cases, it is even possible to arrange materials in a cyclic triboelectric series. For example, in the list {glass, zinc, silk, filter paper, cotton, glass} each material attracts negative charge during rubbing from that standing to its immediate left [33].

The existence of cyclic triboelectric series implies that tribocharging between dielectrics cannot generally be rationalized in terms of unique or effective electron affinities and ionization energies of the involved (free-standing) dielectrics. However, it may be premature to conclude that the existence of cyclic triboelectric series can only be explained by ion transport as argued previously [32]. Local pressures at points of intimate mechanical contact can be very high for brief moments, i.e., shorter than the time needed to nucleate a dislocation. Consequently, local stresses can reach the theoretical yield stress of the underlying materials for times sufficiently long for electron transfer reactions to take place. During the time interval when pressures are extreme, hybridization changes and/or the generation of charged molecules can occur in a tribological contact [34,35], and dramatically altered charge transfer characteristics may result.

The model used in this work is too crude to reflect hybridization effects, surface gap states or other effects whose descriptions would necessitate sophisticated parameterization schemes. However, this deficiency is not intrinsic to the idea of assigning oxidation states to atoms, but rather a consequence of restricting the parameterization to two-body terms. In our approach, positive charge tends to flow from the electronegative to the electropositive material, and, as far as mono-atomic solids are concerned, the model would result in a well-defined triboelectric series.

Apart from this limitation, the redoxSQE approach introduced in this work can reproduce qualitative features of the charge transfer between two dielectrics, as shown in Figure 6. Charge can be exchanged between two contacting solids or clusters. Unlike those placed onto a metal, charges being donated to a dielectric do not spread out over the surface but remain pinned near the point of contact. This behavior would also be found in real systems, except that electrons would be allowed to hop on long time scales. This, in principle, could have been incorporated in the simulations as well.

Although the atomic hardnesses for the contact formation between two dielectrics chosen the same as those

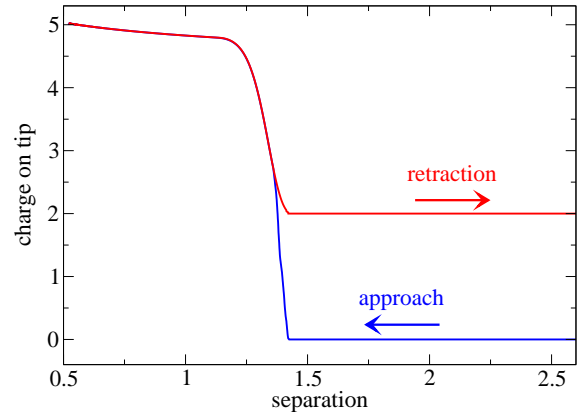


Fig. 7. Charge of the electropositive dielectric tip from Figure 6 as a function of separation during approach and retraction in the redoxSQE model.

used in the simulation of metal clusters, the total amount of transferred charge is much less, which can be seen when comparing Figure 7 to Figure 5. Since ICTs are only attempted between the two front atoms of the tip with the closest substrate atoms, and not passed on further within the cluster, the charge that is ultimately transferred is restricted to two elementary charges for the given set up. In comparison, the number of transferred elementary charges is 13 for the two studied metal clusters. Another difference is that polarization charge in the dielectric is located near the atoms with non-zero oxidation number, while it is spread much more evenly across the metal surface.

3.3 Semi-quantitative considerations

The two examples of contact electrification discussed above do not pertain to any particular material. However, they reflect reality in the sense that collectivity induces the possibility to transfer integer charges between (SQE) materials, even if the atoms constituting the electropositive material have an ionization energy I exceeding the electron affinity A of the atoms composing the counter body. In this section, we expand the analysis of how collectivity affects the values for I and A within the redoxSQE model — and thus redox characteristics — in two specific systems, namely adsorbed atoms on metals and water molecules near an NaCl dimer.

In a pioneering work almost 80 years ago, Gurney [36] discussed why the work function of tungsten can be reduced through a few alkaline earth atoms. He argued that this observation cannot be explained in a classical picture since ionizing, say, a single Ca atom costs $I_{\text{Ca}} \approx 6.1$ eV, which exceeds the work function of tungsten $W_{\text{W}} \approx 4.5$ eV. Yet, redoxSQE reproduces the observed experimental trend. Given that all bonds are metallic (the argument remains unchanged if the redoxSQE bond between Ca and W has a large but finite polarizability), charge can be shared among different (isolated) Ca atoms on the surface. This diminishes the effect of the atomic hardness, and electronegativity becomes the relevant parameter, i.e., $\chi_{\text{Ca}} =$

1 V. Since values for χ differ only slightly between alkaline and alkaline earth metals, in contrast to their ionization energies, redoxSQE finds a similar reduction in W_W for alkaline and alkaline earth adsorbates, in agreement with the observations reported in reference [36].

For the adsorbed metals, ionization potentials were reduced because new dielectric or metallic bonds allowed to spread the charge. External potentials can also achieve such a reduction, as we now discuss. Without hydration, a NaCl dimer dissociates in its ground state into two neutral atoms because $I_{\text{Na}} \approx 5$ eV is greater than the electron affinity of chlorine, $A_{\text{Cl}} \approx 3.6$ eV. In order to estimate the effect of hydration for the dissociated dimer, let us assume that electrostatic interactions are dominant at a separation of $r = 2.5$ Å between a water molecule and an ion of integer charge. The electrostatic potential of a dipole is $\Phi = \mathbf{d} \cdot \mathbf{r} / (4\pi\epsilon_0 r^3)$. Thus the energy gain for a perfectly oriented dimer \mathbf{d} is $\Delta E = dr / (8\pi\epsilon_0 r^2)$. Inserting $d = 1.85$ debye (the value for an isolated H₂O molecule) yields $\Delta E \approx 0.4$ eV for singly charged ions. Thus, approximately two water molecules per ion are sufficient to topple the energy balance toward a charged dissociation limit. We conclude that redoxSQE, once well parameterized, would find — and remember! — that rock salt molecules decompose into neutral atoms in an inert-gas atmosphere but as ions in a sufficiently polar solvent, although the latter screens the direct Coulomb interaction between the ions.

4 Discussion and Conclusions

In this paper, we showed that introducing formal oxidation states to the split charge model allows one to reproduce various generic charge transfer features that occur during the contact formation and breaking of two solid clusters. The main idea behind the approach is that oxidation states of atoms can only change via a redox reaction involving two or more nearby atoms. This way partial charges are neither automatically constant nor a well-defined function of the instantaneous configuration but may be history dependent.

An important many-body effect implicitly contained in the model is that integer charge transfer can occur between two dielectrics of different electron affinity. This happens even though breaking (adiabatically) any molecule consisting of two (stable) atoms in an inert environment automatically results in two neutral atoms, at least for realistic values of their atomic hardnesses and electronegativities. The reason for this behavior lies in a reduced ionization energy I for collective systems in comparison to isolated atoms. In a future publication, we will demonstrate that the methodology explored in this work moreover reproduces a variety of generic features that occur during the discharge and the aging of batteries [4]. No currently popular force field can achieve this, because they all assume a one-to-one correspondence between atomic coordinates and interatomic forces. Time-dependent density functional theory approaches are likewise likely to fail to produce such features due to the serious constraints on particle numbers and simulation times.

Our case study reproducing the generic features of contact-induced charging between two dielectrics assumes implicitly that electric current is effected by the passage of integer charges, i.e., electrons, from one solid to the other. We nevertheless do not intend to take sides in the discussion of what charge types are mainly responsible for charge transfer [30,32]. Protons, hydroxides, or other ions might be equally or even more important than electrons. Our purpose is to provide a formalism with which this issue can be addressed in terms of many-atom, force-field based simulations. This includes the ability to ascertain whether an atom leaves a solid or a cluster as a neutral atom or as an ion. Moreover, the redoxSQE method allows for the (local) electron or ion exchange between stoichiometrically similar materials, as long as local properties materials are distinct, e.g., because of chemical heterogeneity or different local radii of curvature. Thus, there is a chance to identify reasons for the frequently observed charge transfer between chemically identical materials. Of course, recognizing the main mechanism of contact electrification for a specific system requires a realistic and chemistry-specific parameterization.

It is encouraging that the original SQE formalism reproduces fractional charges and polarizabilities quite accurately for systems in which atoms have a well-defined oxidation state [8,10,13,12,18,20,17]. Moreover, it has been shown that the reactant and the product of a redox reaction, namely terminally blocked and zwitterionic pentalanine, can be described quite accurately if the functional groups are subjected to constraints [20]. The effects of the constraints are very similar to those induced by assigning discrete oxidation states to atoms. We are thus confident that it is possible to describe products and reactants of redox reactions reasonably well within one unified framework, although it might be necessary to define (effective) chemical hardness values for all relevant oxidation states.

What still has to be achieved, however, is a way to assign reasonable rates for the redox reactions, in particular near the transition state. In this context it needs to be mentioned that our classical description of an isolated diatomic molecule produces a zero gap between ground state and first excited state at the transition state. This violates the non-crossing rule of quantum mechanics [37].

As for any coarse-graining effort, the important question is whether the information lost is relevant to the problem of interest. To answer this question, we first note that coarse-graining — as we do it here implicitly from a full quantum-mechanical description of the electronic structure to partial charges and oxidation states — must entail loss of information, unless the full description is not optimal. As a benefit, larger systems and longer time scales become accessible. Second, most experiments studying contact charging between dielectrics [30,32], in particular those where electron hopping in the dielectrics are negligible, find that the rate of withdrawal of the surfaces barely affects the final charge. This observation can be rationalized quite easily by noticing that the tunneling rate of electrons or the transfer rates of ions decrease roughly exponentially with the distance between two solids. Last

but not least, in the all-atom battery simulations that will be presented in a future publication, we find that both cut-off r_1 and the rate of trial integer-charge transfer moves do not change results within the statistical error bars. We therefore conclude that it should indeed be possible to parameterize redoxSQE for many applications in such a way that the outcome of the simulations produce the correct ensemble average, e.g., accurate distributions of charge transfer between colliding clusters or rubbing solids.

We thank the Jülich Supercomputing Centre for computing time and Razvan Nistor and Ling Ti Kong for useful discussions. Also, we thank Michael Springborg and Jorge Vargas for assistance with the MP2 calculations.

References

1. S. W. Rick and S. J. Stuart. *Rev. Comp. Chem.*, 18:89, 2002.
2. P. E. M. Lopes, B. Roux, and A. D. MacKerell, Jr. *Theor. Chem. Acc.*, 124:11–28, 2009.
3. M. A. L. Marques, C. A. Ullrich, F. Nogueira, A. Rubio, K. Burke, and E. K. U. Gross. *Time-Dependent Density Functional Theory*. Springer, Heidelberg, 2006.
4. W. B. Dapp and M. H. Müser. (submitted).
5. K. D. Nielson, A. C. T. van Duin, J. Oxgaard, W. Q. Deng, and W. A. Goddard. *J. Phys. Chem. A*, 109:493–499, 2005.
6. V. May and O. Kühn. *Charge and Energy Transfer Dynamics in Molecular Systems*. Wiley-VCH, Weinheim, 2011.
7. M. H. Müser. *Eur. Phys. J. B*, 85:135, 2012.
8. R. A. Nistor, J. G. Polihronov, M. H. Müser, and N. J. Mosey. *J. Chem. Phys.*, 125:094108, 2006.
9. R. A. Nistor and M. H. Müser. *Phys. Rev. B*, 79:104303, 2009.
10. D. Mathieu. *J. Chem. Phys.*, 127:224103, 2007.
11. G. L. Warren, J. E. Davis, and S. Patel. *J. Chem. Phys.*, 128:144110, 2008.
12. T. Verstraelen, V. Van Speybroeck, and M. Waroquier. *J. Chem. Phys.*, 131:044127, 2009.
13. P. T. Mikulski, M. T. Knippenberg, and J. A. Harrison. *J. Chem. Phys.*, 131:241105, 2009.
14. W. J. Mortier, K. van Genechten, and J. Gasteiger. *J. Am. Chem. Soc.*, 107:829, 1985.
15. R. G. Parr and R. G. Pearson. *J. Am. Chem. Soc.*, 105:7512, 1983.
16. P. Itskowitz and M. L. Berkowitz. *J. Phys. Chem. A*, 101:5687, 1997.
17. M. T. Knippenberg, P. T. Mikulski, K. E. Ryan, S. J. Stuart, G. T. Gao, and J. A. Harrison. *J. Chem. Phys.*, 136:164701, 2012.
18. T. Verstraelen, S. V. Sukhomlinov, V. Van Speybroeck, M. Waroquier, and K. S. Smirnov. *J. Phys. Chem. C*, 116:490–504, 2012.
19. T. Verstraelen. (personal communication).
20. T. Verstraelen, E. Pauwels, F. De Proft, V. Van Speybroeck, P. Geerlings, and M. Waroquier. *J. Chem. Theo. Comp.*, 8:661–676, 2012.
21. S. M. Valone. *J. Chem. Theo. Comp.*, 7:2253, 2011.
22. S. M. Valone. *J. Phys. Chem. Lett.*, 2:2618, 2011.
23. D. G. Pettifor and I. I. Oleinik. *Phys. Rev. B*, 59:8487, 1999.
24. M. J. Frisch, G. W. Trucks, H. B. Schlegel, G. E. Scuse-ria, M. A. Robb, J. R. Cheeseman, J. A. Montgomery, Jr., T. Vreven, K. N. Kudin, J. C. Burant, J. M. Millam, S. S. Iyengar, J. Tomasi, V. Barone, B. Mennucci, M. Cossi, G. Scalmani, N. Rega, G. A. Petersson, H. Nakatsuji, M. Hada, M. Ehara, K. Toyota, R. Fukuda, J. Hasegawa, M. Ishida, T. Nakajima, Y. Honda, O. Kitao, H. Nakai, M. Klene, X. Li, J. E. Knox, H. P. Hratchian, J. B. Cross, V. Bakken, C. Adamo, J. Jaramillo, R. Gomperts, R. E. Stratmann, O. Yazyev, A. J. Austin, R. Cammi, C. Pomelli, J. W. Ochterski, P. Y. Ayala, K. Morokuma, G. A. Voth, P. Salvador, J. J. Dannenberg, V. G. Zakrzewski, S. Dapprich, A. D. Daniels, M. C. Strain, O. Farkas, D. K. Malick, A. D. Rabuck, K. Raghavachari, J. B. Foresman, J. V. Ortiz, Q. Cui, A. G. Baboul, S. Clifford, J. Cioslowski, B. B. Stefanov, G. Liu, A. Liashenko, P. Piskorz, I. Komaromi, R. L. Martin, D. J. Fox, T. Keith, M. A. Al-Laham, C. Y. Peng, A. Nanayakkara, M. Challacombe, P. M. W. Gill, B. Johnson, W. Chen, M. W. Wong, C. Gonzalez, and J. A. Pople. *Gaussian 03, Revision C.02*. Gaussian, Inc., Wallingford, CT, 2004.
25. M. Born and J. E. Mayer. *Z. Phys.*, 75:1–18, 1931.
26. A. R. Oganov, M. J. Gillan, and G. D. Price. *J. Chem. Phys.*, 118:10174–10182, 2003.
27. J. S. Reparaz, L. R. Muniz, M. R. Wagner, A. R. Goni, M. I. Alonso, A. Hoffmann, and B. K. Meyer. *Appl. Phys. Lett.*, 96:231906, 2010.
28. J. C. Tully. *J. Chem. Phys.*, 93:1061–1071, 1990.
29. J. Lowell and A. C. Rose-Innes. *Adv. Phys.*, 29:947, 1980.
30. A. F. Diaz and R. M. Felix-Navarro. *J. Electrostatics*, 62:277–290, 2004.
31. C. M. Mate. *Tribology on the small scale*. Oxford University Press, Oxford, 2008.
32. L. S. McCarthy and G. M. Whiteside. *Angew. Chem. Int. Ed.*, 47:2188–2207, 2008.
33. W. R. Harper. *Contact and frictional electrification*. Laplacian Press, Morgan Hill, 1998.
34. N. J. Mosey, M. H. Müser, and T. K. Woo. *Science*, 307:1612, 2005.
35. N. J. Mosey, T. K. Woo, and M. H. Müser. *Phys. Rev. B*, 72:054124, 2005.
36. R. W. Gurney. *Phys. Rev.*, 47:479–482, 1935.
37. J. von Neumann and E.P. Wigner. *Z. Physik*, 30:467, 1929.